Journal of Power Sources 186 (2009) 286–292

Contents lists available at ScienceDirect

Journal of Power Sources

journal homepage: www.elsevier.com/locate/jpowsour

Hybrid acid–base polymer membranes prepared for application in fuel cells

Dan Wu, Tongwen Xu*, Liang Wu, Yonghui Wu

Laboratory of Functional Membranes, School of Chemistry and Materials Science, University of Science and Technology of China (USTC), Hefei, Anhui 230026, People's Republic of China

ARTICLE INFO

Article history:
Received 22 July 2008
Received in revised form 7 October 2008
Accepted 7 October 2008
Available online 18 October 2008

Keywords:
Fuel cell
Proton-exchange membrane
Hybrid
Acid–base
SPPO

ABSTRACT

For application in fuel cells, a series of hybrid acid–base polymer membranes were prepared by blending sulfonated poly(2,6-dimethyl-1,4-phenylene oxide) (SPPO) with (3-aminopropyl)triethoxysilane (A1100) through a sol–gel process. As indicated by scanning electron microscopy, energy-dispersive X-ray analysis, and thermogravimetric analysis, the acid–base interaction improves not only the membrane homogeneity and thermal stability but also the mechanical strength and flexibility. Apart from the low cost, the developed membranes exhibit high proton conductivity and low methanol permeability as compared to Nafion® 117. Further, the optimal membrane shows better performance than Nafion® 117 in a single cell test. All these properties make the hybrid membranes suitable for application in fuel cells.

1. Introduction

Proton-exchange membrane fuel cells (PEMFCs) are considered one of the most promising alternatives to internal combustion engines due to their fuel renewability (hydrogen, methanol, ethanol, etc.), high efficiency, and environmental compatibility [1–5]. Hydrogen PEMFCs were studied the most extensively because of their high efficiency and relatively easy operation on the fuel cell itself, and broad allowable temperatures [3–5]. A series of perfluorosulfonate ionomers, such as Nafion®, are often used as proton-exchange membranes in PEMFCs because of their high proton conductivity, and excellent chemical and physical properties; however, high cost and high fuel crossover as well as other problems have limited their practical use in fuel cell applications [6,7]. To date, many studies have been carried out to develop alternative membranes with good fuel cell performance and low cost [6,8–12].

Among those alternatives, acid–base polymer blends are promising materials [2,10,13–16]. The interactions between acid and base polymers, such as ionic cross-linking (electrostatic forces) and hydrogen bonding bridges, contribute markedly to the control of membrane swelling without a decrease in flexibility. Therefore, these membranes have low water uptake, reduced crossover, high proton conductivity, good thermal stability, and high mechanical flexibility and strength.

Conversely, organic–inorganic hybrid membranes have also attracted considerable attention from fuel cell developers [14,17–20] because the introduction of inorganic components to organic membranes through a sol–gel process can improve the mechanical and thermal properties as well as proton conductivity. Sometimes, however, the rigidity of the inorganic component makes the resulting membrane brittle.

For application in fuel cells, the above two concepts are combined in this study and a series of hybrid acid–base polymer membranes are prepared by blending sulfonated poly(2,6-dimethyl-1,4-phenylene oxide) (SPPO) with (3-aminopropyl)triethoxysilane (A1100) through a sol–gel process. SPPO is a flexible polymer with the aryl ether backbone and possesses electrochemical properties owing to the pendant sulfonic acid groups [21,22]. Nonetheless, it is highly hydrophilic and may swell strongly in water when the degree of sulfonation is above 28% (and the corresponding ion exchange capacity (IEC) is about 2 meq g^{-1}). The dimensional instability prevents SPPO from practical applications in fuel cells. If SPPO is blended with A1100, acid–base interactions (ionic cross-linking and hydrogen bonding bridges) will be formed between the organic component (SPPO) and the inorganic component (A1100), which can prevent silica from agglomerating to some degree and can result in flexible membranes.

Therefore, a series of flexible hybrid proton-exchange membranes for fuel cells were developed by blending SPPO and A1100 in this study. The formation and effect of acid–base interaction will be discussed in detail. Properties related to fuel cell applications, especially the hydrogen fuel cell performance of the resulting membrane, will be evaluated.

* Corresponding author. Tel.: +86 551 3601587; fax: +86 551 3601592.
E-mail address: twxu@ustc.edu.cn (T. Xu).

0378-7753/$ – see front matter © 2008 Elsevier B.V. All rights reserved.
doi:10.1016/j.jpowsour.2008.10.028

2. Experimental

2.1. Materials

Poly(2,6-dimethyl-1,4-phenylene oxide) (PPO) of intrinsic viscosity equal to 0.57 dl g^{-1} in chloroform at 25 °C was supplied by Institute of Chemical Engineering of Beijing (China). (3-aminopropyl)triethoxysilane (99%) was purchased from Aldrich®. Chlorosulfonic acid, chloroform, *N*,*N*-dimethylformamide (DMF), and other chemicals were of analytical grade. SPPO was prepared by sulfonation of PPO according to the literature [23]. The IEC value of the obtained SPPO was 2.52 meq g^{-1}.

2.2. Membrane preparation

SPPO in the Na^+ or H^+ form was dissolved in DMF (1 g SPPO in 3 ml DMF). A1100 and deionized water with a molar ratio of 1:3 were mixed together in DMF. These two solutions were blended and stirred for 1 h to prepare a uniform membrane solution. The membranes were formed by casting the membrane solution onto a Teflon plate and then evaporating the solvent at 50 °C for 24 h. Then, the membrane was heated at 70 °C for 6 h, 90 °C for 3 h, and 110 °C for 2 h by turn. All the resulting membranes were treated with 1 N HCl aqueous solution for 48 h at room temperature, and the HCl aqueous solution was replaced with a fresh one after 24 h. Finally, the membranes were washed with deionized water and stored in deionized water before use.

2.3. Membrane characterization

2.3.1. Membrane morphologies and thermogravimetric analysis (TGA)

Before tests, the membrane samples were dried at 50 °C under vacuum for 24 h. To observe the membrane morphologies, the samples were quenched in liquid nitrogen and then the fracture surface was observed using scanning electron microscopy (SEM) (XT30 ESEM-TMP PHILIPS). Simultaneously, the elemental distributions along the thickness direction were analyzed by energy-dispersing X-ray analysis (EDXA).

The thermal behaviors of membranes were determined by thermogravimetric analyzer (TGA-50H, Shimadzu) in 20 ml min^{-1} nitrogen atmosphere with a heating rate of 10 °C min^{-1}.

2.3.2. Ion exchange capacity (IEC)

Initially, the membrane sample in the H^+ form was soaked in 0.5 mol l^{-1} NaCl solution for 24 h. Then, the sample was taken out and washed with deionized water. The water used for washing was collected and mixed with the remaining solution. This mixture solution was titrated with a 0.01 mol l^{-1} NaOH standard solution. The IEC value was calculated according to the following equation:

$$\mathrm{IEC} = \frac{V_{\mathrm{NaOH}} \times C_{\mathrm{NaOH}}}{w_{\mathrm{dry}}} \quad (1)$$

where w_{dry} is the dry weight of the sample in the H^+ form, V_{NaOH} is the titrated volume of the NaOH solution, and C_{NaOH} is the concentration of the NaOH solution (0.01 mol l^{-1}).

2.3.3. Water uptake and swelling ratio

The membrane sample in the H^+ form was soaked in deionized water at room temperature for 24 h. After becoming completely swollen, the sample was taken out, wiped with a tissue paper to remove the excess water, and weighed immediately. The wet sample was dried at 50 °C under vacuum until the constant weight was reached. The water uptake *W* was calculated according to the following equation:

$$W = \frac{w_{\mathrm{wet}} - w_{\mathrm{dry}}}{w_{\mathrm{dry}}} \times 100\% \quad (2)$$

where w_{wet} and w_{dry} are the wet and dry weights of the sample, respectively.

The swelling ratio was characterized by linear expansion ratio (LER), which was determined by the difference between wet and dry dimensions of a membrane sample (3 cm in length and 1 cm in width). The calculation was based on the following equation:

$$\mathrm{LER} = \frac{L_{\mathrm{wet}} - L_{\mathrm{dry}}}{L_{\mathrm{dry}}} \times 100\% \quad (3)$$

where L_{wet} and L_{dry} are the lengths of wet and dry membranes, respectively.

2.3.4. Proton conductivity

The proton conductivity of the membrane was measured using the normal four-point probe technique [12,24]. The membrane samples were in the hydrogen form and fully hydrated. The impedance was determined using an Autolab PGSTAT 30 (Eco Chemie, Netherlands) set at galvanostatic mode with an ac current amplitude of 0.1 mA over the frequency range from 1 MHz to 50 Hz. Using a Bode plot, the frequency region over which the impedance had a constant value was recognized, and the resistance was then obtained from a Nyquist plot. The proton conductivity κ is calculated according to the following equation:

$$\kappa = \frac{L}{RWd} \quad (4)$$

where *R* is the obtained membrane resistance, *L* is the distance between potential-sensing electrodes, and *W* and *d* are the width and thickness of the membrane, respectively.

2.3.5. Crossover

The crossover of the membrane was characterized by methanol permeability. Methanol permeability was measured using a liquid permeation cell, which was composed of two compartments of the same volume (150 ml). Compartment A was filled with a 20 v.% methanol aqueous solution and compartment B was filled with deionized water. Membrane was inserted between these two compartments and the diameter of diffusion area was 1.0 cm. During the permeability measurement, the methanol concentration in compartment B was monitored using a refractive index detector (FI750F, Younglin Instrument). The output signal was converted by a data module (Autochro, Younglin Instrument) and recorded by computer. Methanol permeability *P* was calculated according to the following equation:

$$C_{\mathrm{B}}(t) = \frac{A}{V_{\mathrm{B}}} \frac{P}{d} C_{\mathrm{A}}(t - t_0) \quad (5)$$

where C_A is the initial concentration of the methanol solution in compartment A, $C_B(t)$ is the methanol concentration in compartment B at time *t*, V_B is the volume of deionized water in compartment B, *d* is the membrane thickness, and A is the effective permeating area.

2.3.6. Mechanical testing

The tensile strength and elongation at break of the wet membrane were measured using an Instron universal tester (Model 1185) at 25 °C with dumbbell shape specimens at a crosshead speed of 25 mm min^{-1}. The tensile strength and elongation at break were averages of three tests.

Table 1
Composition and properties of the membranes.

Membrane	Number	A1100 (wt%)	IEC (meq g^{-1})	Water uptake (%)	LER (%)
SPPO-H and A1100	HA-0	0	1.17	21.5	5.95
	HA-5	5	1.34	22.1	5.68
	HA-10	10	1.45	23.4	8.25
	HA-15	15	1.68	30.9	7.81
	HA-20	20	1.52	25.0	8.38
	HA-25	25	1.37	22.8	7.86
SPPO-Na and A1100	SA-0	0	2.52	88.0	27.5
	SA-5	5	2.51	85.7	27.7
	SA-10	10	2.58	89.5	26.8
	SA-15	15	2.45	80.7	21.2
	SA-20	20	2.45	81.9	21.1
	SA-25	25	2.25	74.0	20.8

2.3.7. Installation of membrane electrode assemblies (MEA) and evaluation of fuel cell performances

The catalyst powders (Pt 40 wt%, E-TEK®) and the binder (5 wt% Nafion® solution, Aldrich®) were impregnated into the gas diffusion layers (SIGRACET® GDL 10BC) by a spray technique to prepare the electrodes. The loadings of Pt and Nafion® polymer were 0.4 mg cm^{-2} and 0.13 mg cm^{-2}, respectively. The MEA was fabricated by putting the electrodes on both sides of the wet membrane without hot-pressing. Then, the MEA was mounted into a fuel cell test station with an effective area of 2.2 cm × 2.3 cm. The test was under atmospheric pressure and with a cell temperature of 55 °C. Flow rates of the fuel for anode (pure hydrogen) and the oxidant for cathode (pure oxygen) were both 100 cm^3 min^{-1}. The hydrogen and oxygen were pre-bubbled in distilled water at 55 °C to be moisturized. The fuel cell was loaded at 0.6 V and operated in a constant voltage mode for 12 h by an electrical load equipment (Dae-Gil, Korea). After activation, the current–voltage (I–V) performance of the cell was measured by the same electrical load equipment. The measurement range was between OCV and 0.16 V with a descending rate of 0.02 V s^{-1}.

3. Results and discussion

3.1. IEC, water uptake, and swelling ratio

As described in the experimental section, two series of blend membranes were prepared: (1) the membranes prepared by blending SPPO-H (SPPO in the H^+ form) with A1100, denoted as SPPO-H and A1100 series, and (2) the membranes prepared by blending SPPO-Na (SPPO in the Na^+ form) with A1100, denoted as SPPO-Na and A1100 series. As a reference, a membrane was also prepared with SPPO-H or SPPO-Na alone (without blending) by following the same procedure. The main properties of the membranes, such as IEC, water uptake, and swelling ratio, are listed in Table 1. The starting material SPPO-H has an IEC of 2.52 meq g^{-1}; however, the blank sample (HA-0), which was prepared from only SPPO-H by following the same procedure as that for the other hybrid membranes, was found to have an IEC of 1.17 meq g^{-1}. This is because that some sulfonic acid groups were consumed during the heating treatment in the preparation procedure [25]. After incorporation of A1100, the acid–base interaction between A1100 and SPPO-H protects sulfonic acid groups from consumption. Thus, the IEC values of the hybrid membranes are higher than that the membrane prepared from SPPO-H (HA-0). However, due to an increase in non-charged components (A1100) in the membrane matrix, the IEC values of all the hybrid membranes are lower than that of the starting SPPO-H material (before heating).

As well known, flexible ionomer networks can be built up by mixing polymeric acids and polymeric bases, and the main mechanism is by transferring protons from the acid onto the base and thus forming ionic cross-links [14]:

$$P_1\text{-}SO_3H + P_2\text{-}NR_1R_2 \rightarrow [P_2\text{-}SO_3]^{-+}[HR_1R_2N\text{-}P_2] \quad (6)$$

where P_1 and P_2 are the backbones of the polymeric acid and base, respectively; R_1 or R_2 is hydrogen, alkyl, cycloalkyl, aryl, arylalkyl, etc. It has been reported that such an acid–base complex can be experimentally realized by following two distinctive routes:

The acidic polymers in the H^+ form are directly blended with basic polymers to form the membranes [10,13,15,16].

The acidic polymers in the salt form were blended with basic polymers and then transformed to the H^+ form by acid treatment [13,26].

In our case, SPPO-H was blended with A1100. In the blend, the sulfonic acid group can interact with the amino group of A1100 and form the fully acid–base interaction as follows:

$$PPO\text{-}SO_3H + NH_2\text{-}(CH_2)_3Si(OC_2H_5)_3 \rightarrow [PPO\text{-}SO_3]^{-+}[NH_3\text{-}(CH_2)_3Si(OC_2H_5)_3] \quad (7)$$

As a result, some sulfonic acid groups were protected during the subsequent sol–gel process. This may be the reason why the blend membranes have higher IEC values than SPPO-H blank (HA-0). Meanwhile, as the content of A1100 increases, IEC value increases to 1.68 meq g^{-1} (A1100, 15 wt%) but decreases if the content of A1100 further increases. This is because A1100 does not possess ion exchange capability. When its content reaches some extent, IEC value decreases due to a decrease in the relative weight ratio of SPPO-H. The water uptake has the same changing trend as IEC since IEC indicates the content of sulfonic acid groups in the membrane, which is related to the hydrophilicity. Because of the low water uptake and ionic cross-linking structure, the swelling ratios are at a very low level.

To further elucidate the fact that SPPO-H forms acid–base complexes with A1100, some membranes were prepared with SPPO-Na instead of SPPO-H (SPPO-Na is much more thermally stable than SPPO-H [27,28]). The results are listed in Table 1 for comparison. As shown, the IEC value of SPPO-Na membrane (SA-0) is, as expected, as high as that of the original sulfonated material. The SPPO-Na and A1100 hybrid membranes also possess high IEC values, and only a small decrease occurs when A1100 content is higher than 15%. The water uptake and swelling ratio display the same changing trends as IEC; however, they are much higher than those of SPPO-H and A1100 series. It suggests that the acid–base interaction in the membrane prepared by blending SPPO-Na with A1100 is not enough to restrict the membrane from swelling. Hence, it is better to blend SPPO-H with A1100 to obtain acid–base complexes.

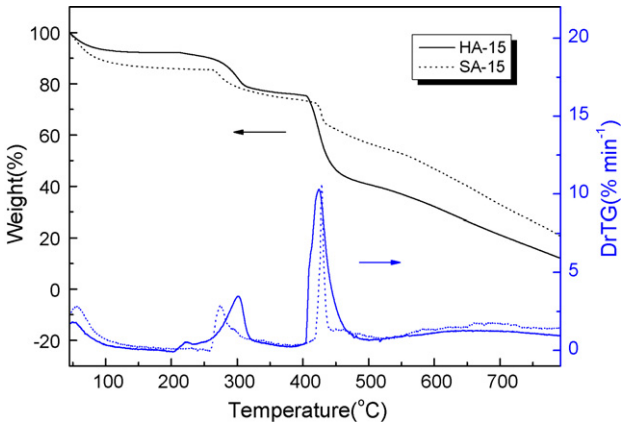

Fig. 1. The thermal stabilities of samples HA-15 and SA-15.

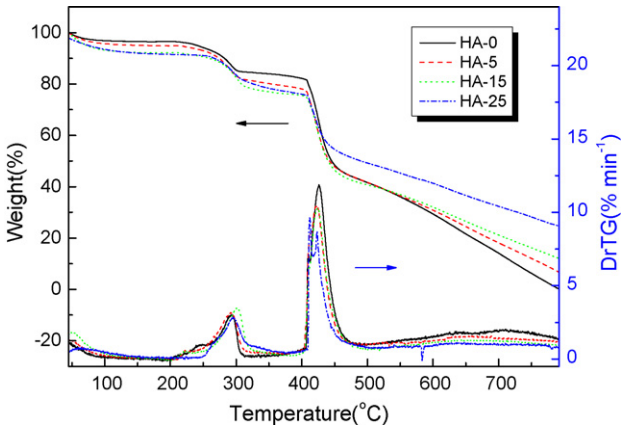

Fig. 2. TG and DrTG of SPPO-H and A1100 membranes.

3.2. Thermal stability

Fig. 1 illustrates the thermal behaviors of HA-15 and SA-15 through TG and DrTG (first order differential of TG to time). The two samples have the same content of A1100 (15 wt%) but are in different forms (SPPO-H and SPPO-Na). The weight loss below 100 °C is attributed to the loss of moisture. In this stage, SA-15 loses more weight than HA-15 due to its high hydrophilicity. The next stage of weight loss is from 210 °C to 350 °C and is ascribed to the decomposition of sulfonic acid groups. The weigh loss of HA-15 starts at 210 °C, and its main decomposition peak is around 300 °C, while SA-15 has only one decomposition peak at around 270 °C. Considering the poor thermal stability of SPPO-H, HA-15 should lose weight first and the substances lost are the sulfonic acid groups which are free from acid–base interaction with A1100. Whereas, the acid–base interaction imparts better thermal stability to the other sulfonic acid groups; hence, its decomposition temperature is even higher than the SPPO-Na in SA-15. This result is consistent

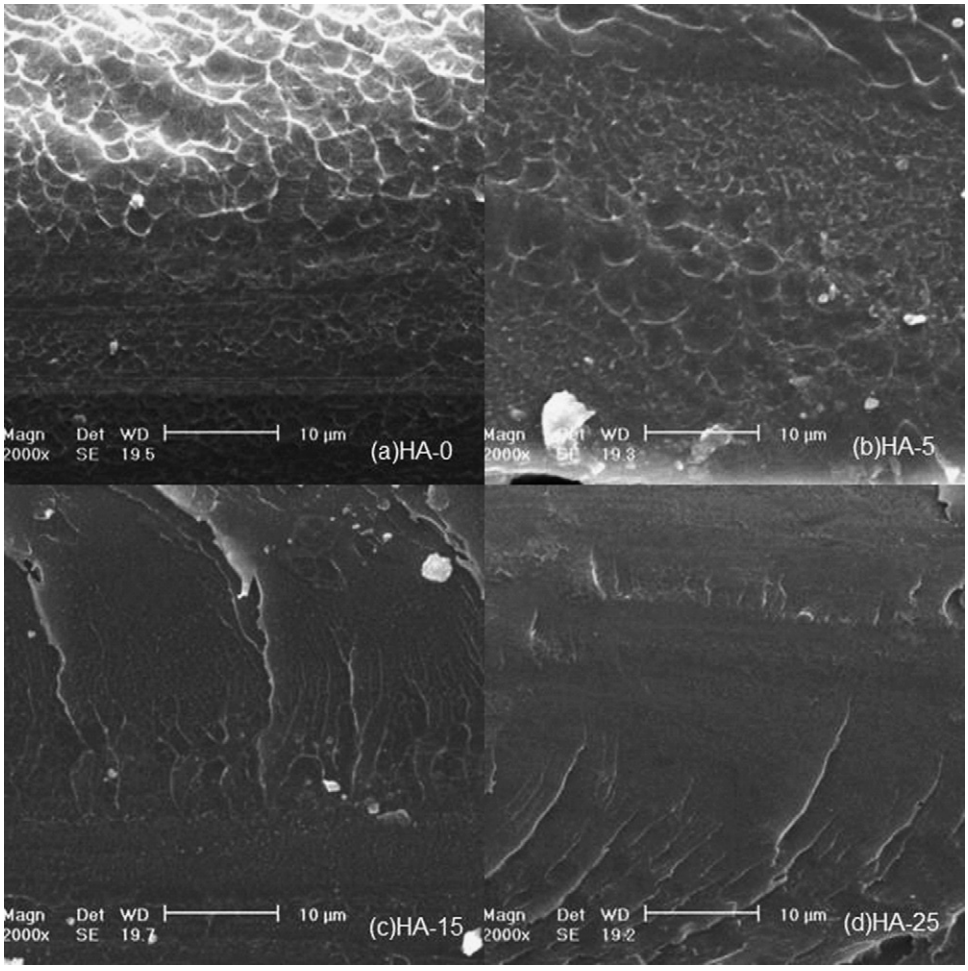

Fig. 3. SEM images of the fracture surfaces of SPPO-H and A1100 membranes.

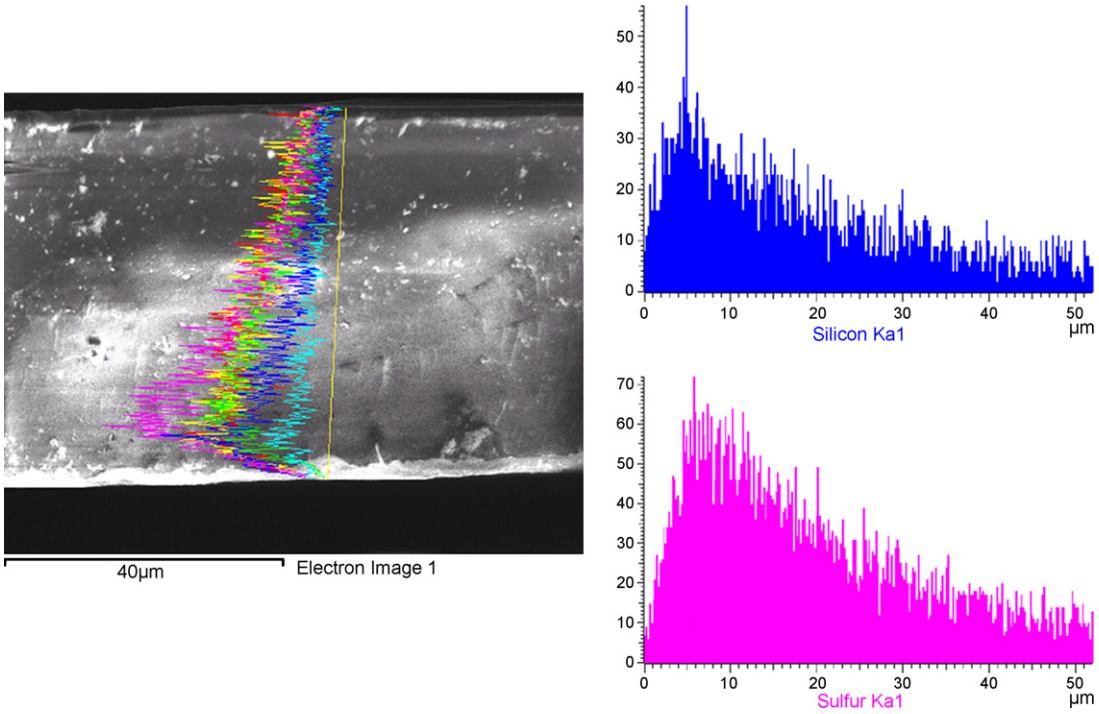

Fig. 4. SEM–EDXA images of the fracture surface of sample SA-15.

with the conclusion concerning the IEC of SPPO-H and A1100 membranes. To sum up, acid–base interaction can protect sulfonic acid groups from decomposition and thus improve the thermal stability of membranes.

The effect of A1100 content was studied by comparing the thermal behaviors of HA-0, HA-5, HA-15, and HA-25. Their TG and DrTG results are illustrated in Fig. 2. Obviously, in the second weight loss stage (decomposition of sulfonic acid groups), the starting temperature increases with an increase in A1100 content. This is because the number of free sulfonic acid groups will decline as A1100 content increases in the membrane. Another notable feature of the TG result is the residual content of silica [29]. As expected, the silica content increases with an increase in A1100 content.

3.3. Morphologies

The membrane morphologies were investigated by examining the fracture surface through SEM. Fig. 3 shows the SEM images of SPPO-H and A1100 membranes. According to the comparison between these four images, the hybrid membrane becomes more homogeneous as A1100 content increases. This phenomenon is very interesting because it differs from the results of most organic–inorganic hybrid membranes [29]. The reason may be as follows: in the case of SPPO-H membrane, the hydrophilic sulfonic acid groups in the pendant and the hydrophobic backbone are agglomerated separately; after introduction of A1100, the acid–base interaction and silica network prevent agglomeration and thus improve the compatibility between the hydrophilic and hydrophobic phases. In general, A1100 contributes to the enhancement on the homogeneity of the hybrid membranes.

The homogeneity of elemental distribution was also examined by SEM–EDXA. Membrane SA-15 is chosen as an example, and the EDXA image of its fracture along the thickness direction is shown in Fig. 4. Silicon and sulfur are distributed along the whole thickness direction, and their contents in the part near the bottom seem a little higher than other parts. This phenomenon also occurs with all the other elements, so it is probably caused by the instrument. In fact, the distributions of silicon and sulfur are uniform in the hybrid membrane, suggesting that the silica network and SPPO polymer are distributed uniformly in the hybrid membrane.

3.4. Proton conductivity and crossover

The proton conductivity is a key property required for fuel cell applications [2]. Fig. 5 shows the proton conductivities of the hybrid membranes and presents a comparison with Nafion® 117. Apparently, SPPO-Na and A1100 series display higher conductivities than Nafion® 117 while SPPO-H and A1100 series show much lower conductivities. According to the vehicular proton conduction mechanism, the protons transport in the form of hydroniums ions [30,31]. So the proton conductivity depends much on the contents of water and sulfonic acid groups. Accordingly, the disparity between the conductivities of these two series can be ascribed to their difference

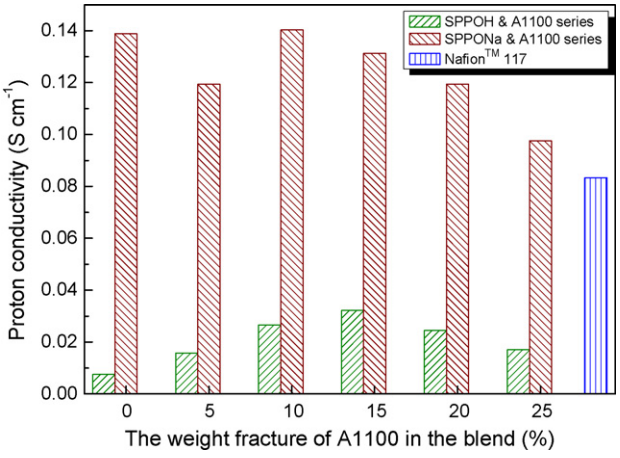

Fig. 5. Proton conductivities of the hybrid membranes and Nafion® 117.

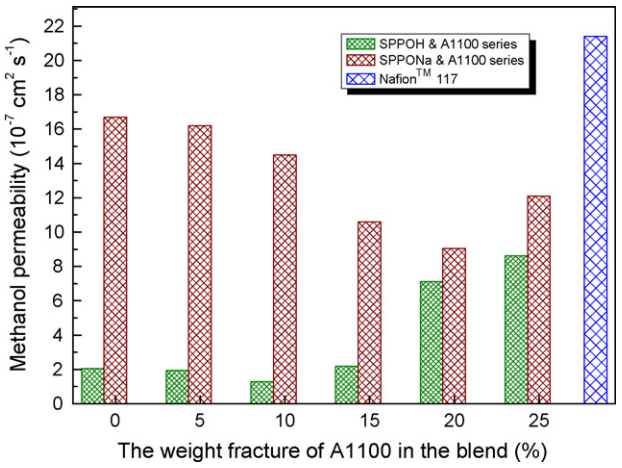

Fig. 6. Methanol permeability of the hybrid membranes and Nafion® 117.

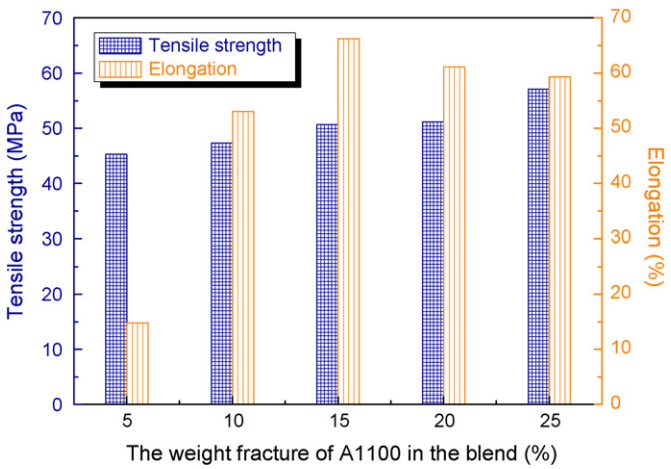

Fig. 7. Tensile strength and elongation at break of the SPPO-H and A1100 membranes.

between IEC values and water uptakes. The relationship between the conductivity difference and A1100 content is almost consistent with the IEC and water uptake results. But it should be noted that silica has a negative effect on the proton transport. So, when A1100 content in the blends reaches to some extent, the proton conductivity decreases.

Fuel crossover reduces fuel cell efficiency, so crossovers of the hybrid membrane with and without A1100 were tested in terms of methanol crossover. Methanol crossover is known to be a major problem in DMFC technology [5,6,31], though no direct methanol fuel cell (DMFC) result is reported here. The methanol permeabilities of these hybrid membranes were measured and are displayed in Fig. 6 in comparison with Nafion® 117. All the hybrid membranes exhibit lower methanol permeabilities than Nafion® 117. That is mainly because the polyphenyleneoxide backbone has no affinity for methanol and the introduction of silica network makes the membrane more compact [12]. In the case of SPPO-H series, the acid–base interaction improves the homogeneity and introduces ionic cross-linking structure; the consumption of sulfonic acid groups during heating results in a cross-linked structure [25]. This membrane structure helps control the methanol crossover. However, when A1100 content is high, the silica agglomerates in the interspaces. As a result, the methanol permeability increases. In the case of SPPO-Na series, the effect of A1100 content shows the same changing trend as SPPO-H series, but the high hydrophilicity leads to the high methanol permeability as compared to SPPO-H series. So, A1100 content is important for the control of methanol crossover. After all, owing to the special membrane structure, SPPO-H and A1100 series performs very low crossover, which provides them positive presumption in fuel cell performance and possibility in DMFC applications.

3.5. Mechanical stability

The mechanical stability of the wet hybrid membranes (SPPO-H and A1100 series) was tested in terms of tensile strength and elongation at break. As presented in Fig. 7, the hybrid membranes show high tensile strength and elongation at break. The tensile strength is enhanced by increasing the content of A1100, which can be attributed to the silica network. Since there is no covalent bond between the polymer and silica, the hybrid membranes remain flexible. Moreover, the results of elongation at break indicate that silica can even improve the flexibility if A1100 content is below 15%. That is probably because the sulfonated polymer is stiff and A1100 prevents polar ionic sites from aggregating [22]. However, when A1100 content increases to some extent, the rigidity of silica plays a dominating role. As a result, the elongation at break slightly decreases when A1100 content is higher than 15%. To sum up, these mechanical properties suggest that the hybrid membranes are strong and flexible.

3.6. Fuel cell test

The hybrid membrane HA-15 (prepared by blending SPPO-H with 15 wt% A1100) was used to evaluate the fuel cell performance. As discussed above, such a membrane has a thickness of 0.083 mm, proton conductivity of 0.0723 S cm^{-1}, water uptake of 30.9%, good mechanical properties, and low methanol permeability. The single cell employing the membrane was fed with humidified pure hydrogen and oxygen to the anode and cathode, respectively, and was operated at 55 °C. After activation, the I–V performance of the cell was recorded and is shown in Fig. 8 in comparison with Nafion® 117.

As shown in Fig. 8, the cell using the hybrid membrane exhibits a slightly lower open circuit voltage (OCV) (930 mV) as compared to the cell using Nafion® 117 (980 mV). This is mainly because there is a difference in thickness between the hybrid membrane (0.083 mm) and Nafion® 117 (0.198 mm) and the thickness plays a leading role in determining the permeation, which influences the OCV [32]. Nonetheless, all the other performances of the hybrid membrane

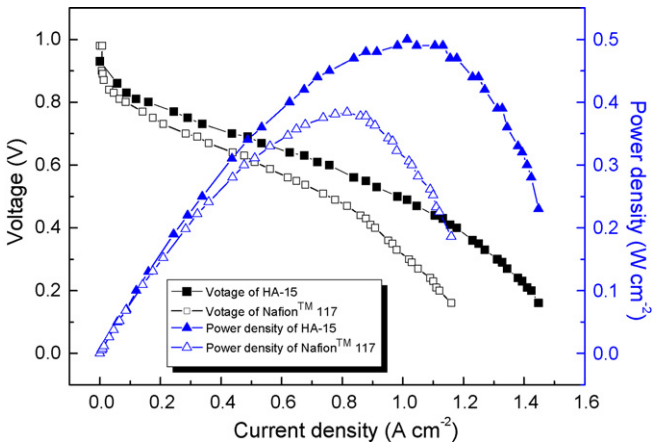

Fig. 8. Single cell polarization curves of the hybrid membrane HA-15 and Nafion® 117.

are better than those of Nafion® 117. At a given voltage, the cell using the hybrid membrane exhibits larger current density than that of the cell using Nafion® 117. The maximum power density of the cell using the hybrid membrane is 0.50 W cm^{-2} at a current density of 1.014 A cm^{-2}, while that of Nafion® 117 is 0.384 W cm^{-2} at a current density of 0.816 A cm^{-2}. These results suggest that the hybrid membrane has a great potential for application in fuel cells.

4. Conclusions

A series of hybrid acid–base polymer membrane were prepared from blends of SPPO and A1100. The acid–base interaction proved effective to improve the thermal stability, homogeneity, and dimensional stability of the membrane. Moreover, this interaction between the organic and inorganic components makes the resulting membranes higher in mechanical strength and flexibility. These low cost membranes possess high proton conductivity and low methanol permeability. Especially, the single cell test indicates that these membranes are competitive with Nafion® 117. All these properties make the hybrid membranes suitable for fuel cell applications.

Acknowledgements

This research was financially supported by the National Science Foundation of China (No.20636050), the NSFC-KOSEF Scientific Cooperation Program (No. 20611140649) and National Basic Research Program of China (No. 2009CB623403). Special thanks will be given to Prof. S.H. Moon for providing the facilities to perform proton conductivity measurement and the single cell test. The authors also thank Mr. C.H. Huang for proofreading the manuscript.

References

[1] M.A. Hickner, H. Ghassemi, Y.S. Kim, B.R. Einsla, J.E. McGrath, Chem. Rev. 104 (2004) 4587–4611.
[2] J. Larminie, A. dicks, Fuel Cell Systems Explained, 2nd ed., John Wiley & Sons Ltd., 2003.
[3] K.D. Kreuer, J. Membr. Sci. 185 (2001) 29–39.
[4] T. Inoue, T. Uma, M. Nogami, J. Membr. Sci. 323 (2008) 148–152.
[5] T. Schultz, S. Zhou, K. Sundmacher, Chem. Eng. Technol. 24 (2001) 1223–1233.
[6] A. Heinzel, V.M. Barragan, J. Power Sources 84 (1999) 70–74.
[7] K.A. Mauritz, R.B. Moore, Chem. Rev. 104 (2004) 4535–4585.
[8] W.C. Choi, J.D. Kim, S.I. Woo, J. Power Sources 96 (2001) 411–414.
[9] A. Kuver, K. Potje-Kamloth, Electrochim. Acta 43 (1998) 2527–2535.
[10] Y.Z. Fu, A. Manthiram, M.D. Guiver, Electrochem. Commun. 9 (2007) 905–910.
[11] B. Smitha, S. Sridhar, A.A. Khan, Macromolecules 37 (2004) 2233–2239.
[12] D. Wu, R.Q. Fu, T.W. Xu, L. Wu, W.H. Yang, J. Membr. Sci. 310 (2008) 522–530.
[13] J. Kerres, A. Ullrich, F. Meier, T. Haring, Solid State Ionics 125 (1999) 243–249.
[14] J.A. Kerres, Fuel Cells 5 (2005) 230–247.
[15] H.L. Wu, C.C.M. Ma, H.C. Kuan, C.H. Wang, C.Y. Chen, C.L. Chiang, J. Polym. Sci. Pt. B: Polym. Phys. 44 (2006) 565–572.
[16] Y.F. Lin, Y.H. Hsiao, C.Y. Yen, C.L. Chiang, C.H. Lee, C.C. Huang, C.C.M. Ma, J. Power Sources 172 (2007) 570–577.
[17] H.Y. Chang, R. Thangamuthu, C.W. Lin, J. Membr. Sci. 228 (2004) 217–226.
[18] J.Y. Kim, S. Mulmi, C.H. Lee, H.B. Park, Y.S. Chung, Y.M. Lee, J. Membr. Sci. 283 (2006) 172–181.
[19] X.J. Cui, S.L. Zhong, H.Y. Wang, J. Power Sources 173 (2007) 28–35.
[20] R.Q. Fu, J.J. Woo, S.J. Seo, J.S. Lee, S.H. Moon, J. Power Sources 179 (2008) 458–466.
[21] T.W. Xu, J. Membr. Sci. 263 (2005) 1–29.
[22] S.F. Yang, C.L. Gong, R. Guan, H. Zou, H. Dai, Polym. Adv. Technol. 17 (2006) 360–365.
[23] T.W. Xu, W.H. Yang, B.L. He, Chem. Eng. Sci. 56 (2001) 5343–5350.
[24] W.F. Chen, P.L. Kuo, Macromolecules 40 (2007) 1987–1994.
[25] S.P.S. Yen, S.R. Narayanan, G. Halpert, E. Graham, A. Yavrouian, US Patent No. 5,795,496 (1998).
[26] K. Bouzek, S. Moravcova, Z. Samec, J. Schauer, J. Electrochem. Soc. 150 (2003) E329–E336.
[27] L. Jia, H. Fu, J. Xu, A. Hirai, H. Odani, J. Appl. Polym. Sci. 52 (1994) 29–37.
[28] R.Y.M. Huang, J.J. Kim, J. Appl. Polym. Sci. 29 (1984) 4017.
[29] S.L. Zhang, C.M. Wu, T.W. Xu, M. Gong, X.L. Xu, J. Solid State Chem. 178 (2005) 2292–2300.
[30] K.D. Kreuer, Chem. Mater. 8 (1996) 610–641.
[31] M. Yamada, I. Honma, Electrochim. Acta 48 (2003) 2411–2415.
[32] X.M. Ren, M.S. Wilson, S. Gottesfeld, J. Electrochem. Soc. 143 (1996) L12–L15.